JOURNAL OF MATERIALS SCIENCE **33** (1998) 4879–4885

Transient creep associated with grain boundary sliding in fine-grained single-phase Al_2O_3

H. YOSHIDA, T. SAKUMA
Department of Material Science, Faculty of Engineering, The University of Tokyo, 7-3-1 Hongo, Bunkyo-ku, Tokyo 113, Japan
E-mail: yoshida@ceramic.mm.t.u-tokyo.ac.jp

Transient creep data for high-purity polycrystalline alumina are examined at the testing temperature of 1150–1250 °C. The data are analysed in terms of the effect of stress and temperature on the extent of transient time and strain.

In order to explain the observed transient creep, a time function of creep strain is proposed from a two-dimensional model based on grain boundary sliding. The grain boundary sliding is assumed to take place by the glide of grain boundary dislocations accommodated by dislocation climb in the neighboring grain boundaries. The time function for a creep strain ϵ obtained from the model is given in a form

$$\epsilon = a_1 t + a_2(1 - \exp(-a_3 t))$$

which is similar to the previous empirical formula describing the experimental creep curves in metallic alloys. The model predicts that the transient creep strain ϵ_T is approximately proportional to and the extent of transient creep time t_T is inversely proportional to flow stress. The prediction is consistent with the experimental data in high-purity, fine-grained alumina at temperatures between 1150 and 1250 °C.

1. Introduction

In high-temperature creep deformation of metals, transient creep usually appears prior to steady state creep [1, 2]. The transient creep has been explained in terms of a transition period of microstructure change during creep which ends up in steady-state.

The constitutive equations for transient creep during dislocation creep in single-phase metals have been derived by many authors. Several authors have tried to explain the observed creep curves from the dislocation density change with time [1, 3–6]. In their analysis, the transient and steady-state creep is described as a linear combination of multiplication and annihilation rates of mobile dislocations, and the transient region is regarded as a stage where the mobile dislocation density is reduced with time. Another model assumes that an evolution of internal stress caused by impediment of dislocation movement and by elastic back stress during transient creep controls creep strain rate, and is an origin of primary and secondary creep curves under various stresses and temperatures [7, 8].

On the other hand, there are several models to describe the transient creep under the condition of diffusional creep [9–13]. For example, Raj [10] showed that the transient behaviour in diffusion creep is caused by the change in grain boundary tractions with time from the initial elastic configuration to the steady-state diffusional configuration.

The transient creep has been observed in fine-grained ceramics as well as metallic materials [14–17]. Chokshi and Porter [15] found the primary creep strains in the order of 1% in four point flexure creep test at 1400 °C in single phase alumina with a grain size of 1.6 μm. Robertson *et al.* [16] also reported the transient creep strain of about 1% in tensile creep testing at 1250 °C in fine-grained Al_2O_3 with a grain size of 1.0 μm. Because dislocation activity is very limited during creep in fine-grained Al_2O_3, either diffusional creep or grain boundary sliding must be responsible for the transient creep. However, it has been pointed out that the transient creep time observed in fine-grained Al_2O_3 at temperature of 1250 °C is much longer than that predicted from the diffusion creep model [16]. Although there is the evidence for grain boundary sliding during creep deformation in fine-grained ceramics [18, 19], strain or time extent of transient creep have not been examined extensively, and the physical basis for the transient creep has not also been given so far.

This paper aims to examine the observed transient creep in fine-grained Al_2O_3, and to propose an equation for high-temperature creep in fine-grained single-phase material on the basis of grain boundary sliding.

2. Experimental procedure

2.1. Material

The material used in this study is fine-grained Al_2O_3 with a purity of 99.99% (TM-DAR, Taimei Chemicals, Tokyo, Japan). The fabrication procedure is described in the earlier papers [20–22]. The sintered Al_2O_3 has

a relative density of more than 99%, and consists of nearly equiaxed grains with a size of 0.9 μm. No glass phase was found in grain boundaries even in high-resolution electron microscopy [23].

2.2. Creep testing

The size of creep specimens was 6×6 mm^2 in cross-section and 8 mm in height. Creep experiments were carried out under uniaxial compression in air at a constant load using a lever-arm testing machine with a resistance-heated furnace (HCT-1000, Toshin Industry, Tokyo, Japan). Applied stresses and temperatures examined are in a range of $10 \sim 160$ MPa and $1150 \sim 1250$ °C, respectively. Test temperature was measured by Pt–PtRh thermocouple attached to each specimen. Test temperature was kept within ± 1 °C.

3. Creep curve and transient creep behaviour

Fig. 1 shows a creep curve (a) and a plot of logarithmic strain rate against time (b) in Al_2O_3 at 1200 °C and the applied stress of 22 MPa. The strain rate becomes nearly constant from a time of about 20 ks which corresponds to $\sim 0.7\%$ strain. The total creep strain, ϵ, at a time t is well described by the following equation

$$\epsilon = a_1 t + a_2(1 - \exp(-a_3 t)) \qquad (1)$$

where the first and second terms indicate steady-state creep strain and transient creep strain, respectively. Equation 1 has the same functional form as that originally proposed by Mcvetty [24], which is extensively

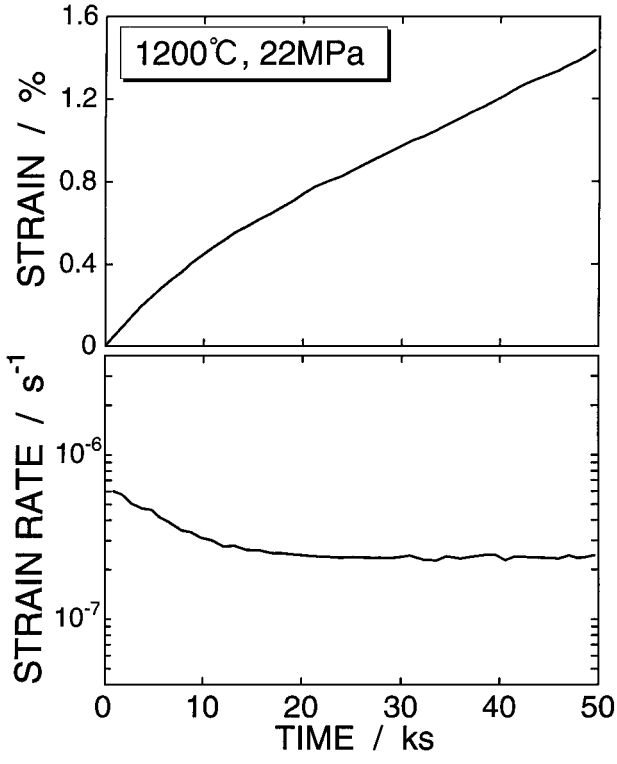

Figure 1 A creep curve in Al_2O_3 (a) and a plot of logarithmic strain rate against time (b) at 1200 °C and the applied stress of 22 MPa. The creep curves show a well defined steady-state stage after a period of transient stage.

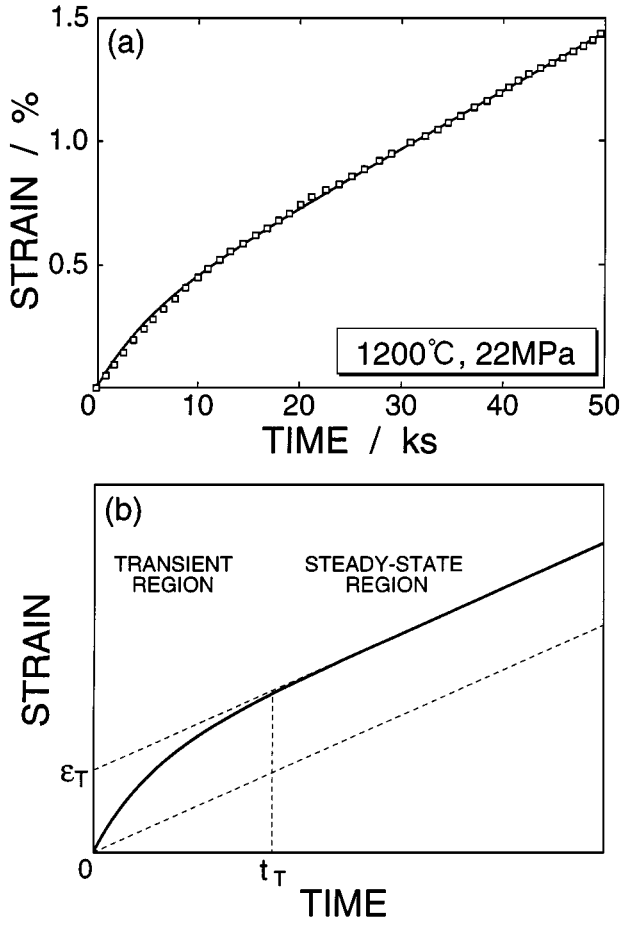

Figure 2 The creep data of Al_2O_3 under an applied stress of 22 MPa at 1200 °C and the fitting line from Equation 1 (a) and the definition of transient creep extent (b).

applicable for creep curve fitting [25]. The value of a_1, a_2 and a_3 are determined from an iteration procedure in which the sum of squares error of the datum points with respect to the average curve is minimized. Fig. 2a is the experimental creep curve and the fitting curve from Equation 1 for a specimen tested at 1200 °C and a stress of 22 MPa. The creep curve is well described by Equation 1. The value of a_1 describes the steady-state strain rate $\dot{\epsilon}_s$, a_2 the total transient strain ϵ_T and a_3 the time extent of transient region. The transient strain is then estimated to be $\sim 0.3\%$ from a plot of Fig. 2b. The value of t_T is estimated to be $-\frac{1}{a_3}\ln(1 - 0.99)$, where the transient creep strain close to the maximum transient strain ϵ_T, and ϵ_T is determined by extrapolating the steady-state creep curve to time zero as illustrated in Fig. 2b.

Fig. 3 shows a log–log plot of t_T against stress, σ in Al_2O_3. It was found that the grain size changes little during creep in this temperature range. At three temperatures, t_T decreases with decreasing applied stress and with increasing testing temperature. The $\log t_T$ against $\log \sigma$ relationship is approximately given by a straight line with a slope of -1 at each temperature. The activation energy for t_T was obtained in a conventional way from an Arrhenius plot of t_T at an applied stress of 53 MPa against inverse temperature in Fig. 4. As shown in this figure, the activation energy of t_T is estimated about 340 kJ mol^{-1}. We consider that the activation

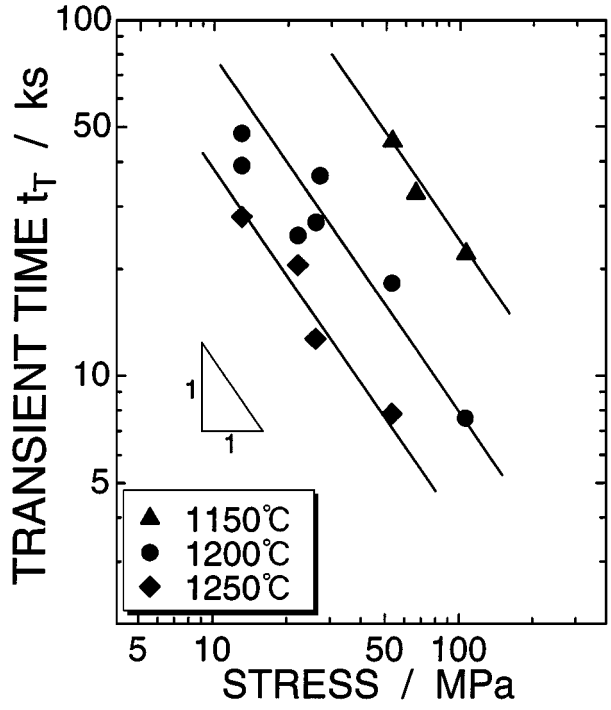

Figure 3 A log–log plot of time extent of transient creep against applied stress in Al_2O_3.

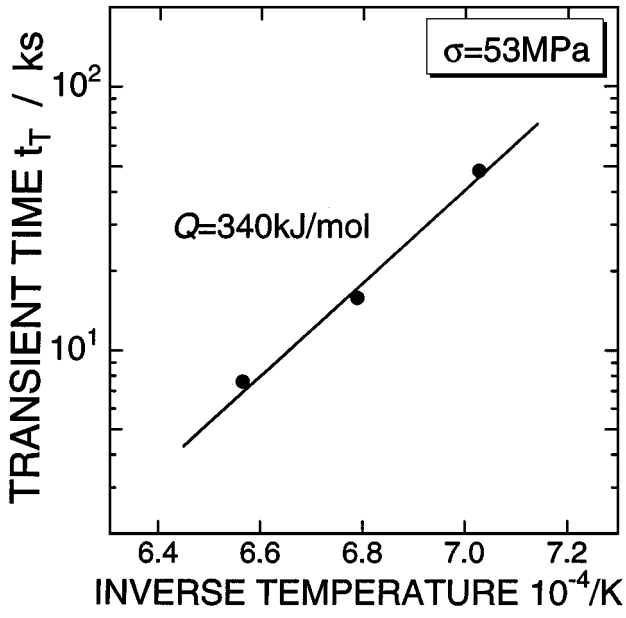

Figure 4 Arrhenius plot of time extent of transient creep against inverse temperature in fine-grained Al_2O_3. The slope of these lines represent the activation energies for time extent of transient creep.

energy obtained from an Arrhenius plot is an approximate value with a tolerance of about 50 kJ mol^{-1}, but the obtained activation energy is nearly similar to the activation energy for grain boundary diffusion of Al^{3+} in Al_2O_3 [26] and is much lower than that for Al^{3+} or O^{2-} ions lattice diffusion; 510 kJ mol^{-1} [27] or 636 kJ mol^{-1} [28]. Fig. 5 is a log–log plot of ϵ_T against σ in Al_2O_3. The plot is a little bit scattered, but ϵ_T can be approximated to be proportional to σ and is rather independent of T.

Malakondaiah *et al.* gave an overview of the transient creep models [12]. Table I [12] shows the dependence

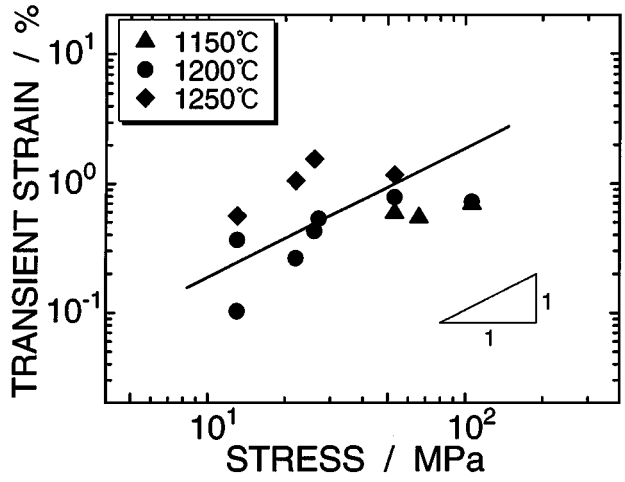

Figure 5 A log–log plot of transient creep strain against applied stress in Al_2O_3.

of transient time and strain on stress and temperature predicted by various models. Except the last two models which assume activity of lattice dislocations, these models can be applicable for fine-grained Al_2O_3, but no models predict the observed dependence of transient time on stress and temperature as shown in Table I. The previous models predict that the transient strain is independent of or inverse proportion to the applied stress, but the present result is also inconsistent with the predictions. One of the possible mechanisms for transient creep in fine-grained Al_2O_3 can be attributed to grain boundary sliding. We will construct the model of transient creep associated with grain boundary sliding in the following section.

4. Analysis

4.1. Description of grain boundary sliding

A rate-controlling mechanism of grain boundary sliding has been considered either from interface reaction controlled diffusion [30, 31] or from dislocation activity in grain boundaries [32–34]. It may be reasonable to assume that grain boundary sliding occurs by dislocation glide in grain boundaries. In a single-phase material, the dislocation glide in grain boundaries will be suppressed at grain boundary corners or ledges where the dislocations are piled up, as shown in Fig. 6a and b, respectively.

Fig. 6a is the situation such that the leading dislocation in the pile-up climbs and dissociates into the two dislocations in the adjacent grain boundary, i.e. they have Burgers' vectors normal and parallel to the grain boundary plane. In the present analysis, the creep deformation is assumed to be controlled by the annihilation of the dislocation with the normal Burgers' vector because of climb in the boundary. The dislocations must diffuse over a distance of $d/4$ along grain boundary to annihilate. In the case of Fig. 6b, dislocation slide must be obstructed by the ledges on grain boundary and the glide distance of a dislocation will be limited by ledge spacing λ and climb distance h.

A formation of the dislocation pile up yields the back stress against gliding dislocation. The remainder of the

TABLE I Dependence of transient time and strain on applied stress and temperature as predicted by various models [12]

Model	Predicted dependence of transient time on		Predicted dependence of transient strain on		Reference
	Stress	Temperature	Stress	Temperature	
Dislocation bowing	Independent	$1/D_l$	Independent	Independent	[13]
Microscopic grain boundary sliding	Independent	$1/D_b$	Independent	Independent	[9]
Lattice diffusion	Independent	$1/D_l$	Independent	Independent	[10]
Grain boundary diffusion	Independent	$1/D_b$	Independent	Independent	[10]
Grain boundaries as sinks for dislocation	$1/\sigma$	$1/D_l$	$1/\sigma$	Independent	[29]
Mutual annihilation of dislocation	Independent	$1/D_l$	$1/\sigma$	Independent	[12]

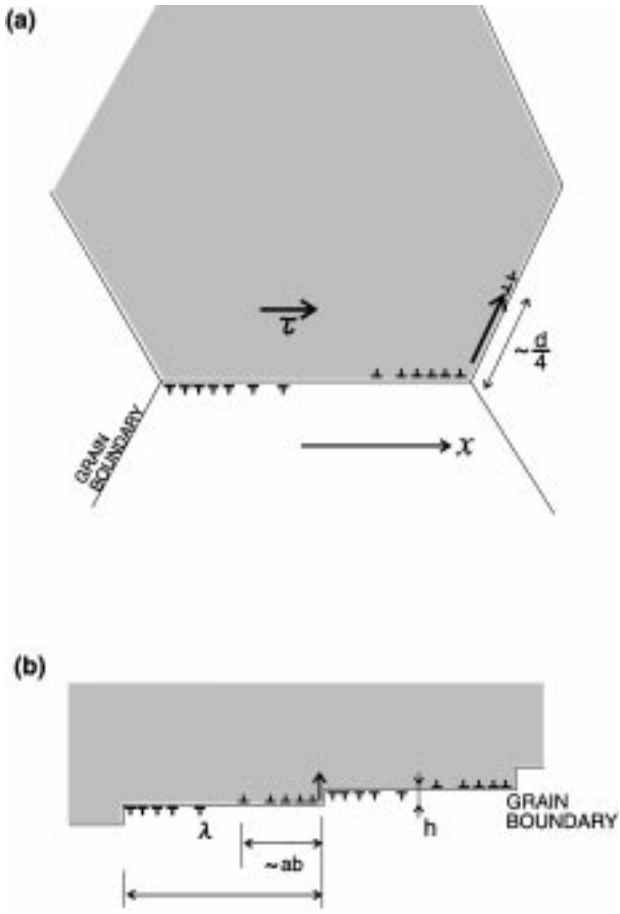

Figure 6 Schematic illustration of grain boundary sliding and its accommodation by grain boundary dislocation activity.

back stress subtracted from applied stress will be the effective stress for the dislocation climb which results in decreasing the rate of grain boundary sliding (i.e. strain hardening). Therefore, the increment of the back stress caused by increased number of pile-up dislocations will reduce the creep rate, while the dislocation climb at the pile up front, will accelerate the creep.

4.2. Grain boundary sliding accommodated by dislocation climb

If the shear strain γ arises from the dislocation glide controlled by climb rate in grain boundaries as described above, the shear strain rate $\dot{\gamma}$ may be described by the rate of climb in the analogy of the climb-controlled shear of lattice dislocations as follows [32]

$$\dot{\gamma} = b\Gamma M\dot{s} \tag{2}$$

where b is the Burgers' vector of grain boundary dislocations, Γ is the area swept out by a dislocation during glide along the grain boundary, M is the number of boundaries per unit volume [1/m^3], and $\dot{s}$ is the frequency of climb of a dislocation (1/s). From the case of Fig. 6a, we can assume that $\Gamma = \frac{\pi}{4}d^2$, and $M = 1/\frac{4}{3}\pi(\frac{d}{2})^3 = 6/\pi d^3$.

The climb frequency $\dot{s}$ under an applied stress of τ is written as

$$\dot{s} = Nb\kappa \tag{3}$$

where N is the length of grain boundary dislocations in an area (m/m^2) and κ is the climb velocity of dislocations (1/s). For simplicity, we use a description $N \sim 2\pi(1-\nu)\tau/\mu b$ [35], which is given by assuming a uniform distribution of dislocations along the boundary, where ν is the Poisson's ratio and μ is the shear modulus.

If a normal stress σ is exerted to edge dislocations in lattice, their climb rate v_y will be given by [35]

$$v_y = \frac{2\pi C_0\Omega^2}{k_{\mathrm{B}}T\ln(L/b)}\frac{D_V}{b}\sigma \tag{4}$$

where C_0 is the concentration of vacancies in local equilibrium (1/m^3), Ω is the vacancy volume, D_V is the diffusivity of vacancy in lattice (m^2 s^{-1}), L is the distance from the dislocation to the region where the vacancy concentration is close to C_0. Following the previous models of superplastic deformation [34], we will use grain boundary diffusion coefficient D_V^{gb} for estimating the climb rate of grain boundary dislocations

$$v_y = \frac{2\pi C_0\Omega^2}{k_{\mathrm{B}}T\ln(L/b)}\frac{D_V^{gb}}{b}\sigma = \frac{d}{4}\kappa \tag{5}$$

Equation 5 yields an apparent climb velocity of

$$\kappa = \frac{D_V^{gb}}{k_{\mathrm{B}}T}\frac{8\pi\Omega^2 C_0}{\ln(L/b)bd}\sigma = \frac{D_b}{k_{\mathrm{B}}T}\frac{8\pi\Omega}{bd\ln(L/b)}\sigma$$

where D_b is the diffusivity equal to $\Omega C_0 D_V^{gb}$ ($m^2\ s^{-1}$). In order to adapt κ to shear components of Equation 2, κ is transformed into a function of shear stress τ as follows

$$\kappa = \frac{D_b}{k_B T}\frac{8q\pi\Omega}{bd\ln(L/b)}(\tau-\tau_b) \sim \frac{D_b}{k_B T}\frac{8(3^{1/2}\Omega)}{bd}(\tau-\tau_b) \tag{6}$$

where q is a converting factor of about $3^{1/2}$ and τ_b is the back stress caused by the dislocation pile up. Substituting Equations 3 and 6 into Equation 2, one obtains

$$\begin{aligned}\dot{\gamma} &= 24(3^{1/2}\pi)(1-\nu)\frac{\Omega}{b^3}\frac{D_b\mu b}{k_B T}\left(\frac{b}{d}\right)^2\frac{\tau(\tau-\tau_b)}{\mu^2}\\ &\equiv A(\tau-\tau_b)\tau\end{aligned} \tag{7}$$

In the case of Fig. 6b, one obtains $\Gamma \sim (\frac{\pi}{4}d^2)(\frac{d}{\lambda})^{-1} = \frac{\pi}{4}d\lambda$ and $M \sim 6/\pi d^2\lambda$ in Equation 2, and $\kappa = v_y/h$. Therefore κ becomes independent of d, and $\dot{\gamma}$ is proportional to d^{-2}. The stress and temperature dependence of $\dot{\gamma}$ is essentially the same with the case of Fig. 6a.

To estimate the back stress τ_b, we will consider a pile up of n edge dislocations in a grain boundary plane under a resolved external stress τ. The dislocation density near the pile up front may be written as $\varrho = 1/ab$, i.e. grain boundary dislocations are present at an interval of ab, where a is a proportionality factor larger than 1. An internal stress between a grain boundary dislocation at x and pile-up dislocations τ_I in the region of $d/4 - nba < x < d/4$ is [35]

$$\begin{aligned}\tau_I(x) &= -\frac{\mu b}{2\pi(1-\nu)}\int_{d/4-nab}^{d/4}\frac{1}{ab}\frac{d\xi}{\xi - x}\\ &= -\frac{\mu}{2\pi a(1-\nu)}[\ln(d/4-x)\\ &\quad -\ln(d/4-nab-x)]\end{aligned} \tag{8}$$

In order for a dislocation to glide from $-d/4$ to $d/4 - nab$, the total work done by τ is

$$\begin{aligned}&\int_{-d/4}^{d/4-nab}\tau_I(x)dx\\ &= -\frac{\mu}{2\pi a(1-\nu)}\left[nab\ln\left(\frac{nab}{d/2-nab}\right)\right.\\ &\quad \left.-\frac{d}{2}\ln\left(\frac{d/2}{d/2-nab}\right)\right]\\ &\sim \frac{n\mu b}{\pi(1-\nu)}\ln\frac{d}{2nab}\end{aligned}$$

and hence the back stress produced by the pile up is given by summation of τ_I as follows

$$\tau_b \sim \frac{n\mu b}{\pi(1-\nu)d}\ln\frac{d}{2nab} \tag{9}$$

The back stress depends on the number of grain boundary dislocations, which is given by the summation of the multiplication rate of mobile dislocations and the annihilation rate caused by dislocation climb. One can write

$$\frac{dn}{dt} = \rho v\alpha - n\kappa \tag{10}$$

where ρ is the dislocation density on a grain boundary ($1/m^2$), v is the glide velocity of a dislocation ($m\ s^{-1}$) and α is a material constant depending on stress and temperature. Taking the Orowan expression for plastic strain rate $\dot{\gamma} = \rho b v$, Equation 10 becomes

$$\begin{aligned}\frac{d\tau_b}{dt} &= \frac{\mu b}{\pi(1-\nu)d}\left(\ln\frac{d}{2nab}-1\right)\left(\frac{\alpha}{b}\dot{\gamma}-n\kappa\right)\\ &\simeq \frac{\mu\alpha}{\pi(1-\nu)d}\ln\frac{d}{2nab}\dot{\gamma} - \kappa\tau_b\\ &\simeq \frac{\zeta\mu\alpha}{\pi(1-\nu)d}\ln\frac{d}{2ab}\dot{\gamma} - \kappa\tau_b\\ &\equiv H\dot{\gamma} - \kappa\tau_b\end{aligned} \tag{11}$$

where ζ is a coefficient ($0 < \zeta < 1$).

By substituting Equation 7 into Equation 11, the time function of τ_b is written as

$$\begin{aligned}\frac{d\tau_b}{dt} &= HA(\tau-\tau_b)\tau - \kappa\tau_b\\ &= HA\tau\left[\tau - \left(1+\frac{\kappa}{HA\tau}\right)\tau_b\right]\\ &\equiv HA\tau(\tau-\theta\tau_b)\end{aligned} \tag{12}$$

where θ is in a range of $(1+\frac{1}{3\zeta\alpha b}\frac{d^2}{\ln d - \ln 2ab}\frac{\tau-\tau_b}{\tau}) \sim (1+\frac{1}{3\zeta\alpha b}\frac{d^2}{\ln d - \ln 2ab})$ under the condition that τ_b is much lower than τ, and θ is nearly independent of temperature and stress. Integration of Equation 12 gives

$$\tau_b = \frac{\tau}{\theta}(1-\exp(-HA\tau\theta t)) \tag{13}$$

By substituting Equation 13 into Equation 7 and integrating, the following equation is obtained

$$\begin{aligned}\gamma &= A\tau^2\left[\left(1-\frac{1}{\theta}\right)t - \frac{1}{HA\tau\theta^2}\exp(-HA\tau\theta t)\right.\\ &\quad \left.+\frac{1}{HA\tau\theta}\right]\\ &= A\tau\left(\tau-\frac{\tau}{\theta}\right)t - \frac{\tau}{H\theta^2}\exp(-HA\tau\theta t) + \frac{\tau}{H\theta}\\ &= A\tau\left(\tau-\frac{\tau}{\theta}\right)t + \frac{\tau}{H\theta^2}[1-\exp(-HA\tau\theta t)]\\ &\quad +\frac{\tau}{HA\tau\theta^2}(\theta-1).\end{aligned} \tag{14}$$

For simple tension, τ, γ and μ are related to the tensile stress σ, strain ϵ and Young's modulus E as follows: $\tau = \sigma/(3)^{1/2}$; $\gamma = 3/2\epsilon$; $\mu = E/2(1+\nu)$.

We will assume $\nu = 0.3$, because $\nu \simeq 0.26 \sim 0.27$ in polycrystalline Al_2O_3 at temperatures of more than 1000 °C [36]. By transforming shear components (γ, τ, μ) into tensile components (ϵ, σ, E), the above equation becomes

$$\epsilon = A\sigma\left(\sigma - \frac{\sigma}{\theta}\right)t + \frac{\sigma}{H\theta^2}[1 - \exp(-HA\sigma\theta t)] + C \tag{15}$$

where C is a constant. This equation gives a time-dependent strain as follows

$$\epsilon = \dot{\epsilon}_s t + \epsilon_T[1 - \exp(-C_1 t)] + C \tag{16}$$

Equation 16 has the same functional form as Equation 1. The transient creep strain ϵ_{tr} is defined by the following equation

$$\begin{aligned}\epsilon_{tr} &= \frac{\sigma}{H\theta^2}[1 - \exp(-HA\sigma\theta t)] \\ &\equiv \epsilon_T[1 - \exp(-HA\sigma\theta t)]\end{aligned} \tag{17}$$

where ϵ_T is the maximum strain of transient creep. The transient strain reaches a saturation strain ϵ_T at an infinite time, but the extent of t_T may be defined as the time up to the transient strain of 99% ϵ_T. We can define the experimentally observable extent of transient creep time such as

$$t_T = -\frac{1}{HA\sigma\theta}\ln(1 - 0.99) \tag{18}$$

5. Discussion

From Equations 17 and 18, stress or temperature dependency of t_T and ϵ_T is approximately given by

$$t_T \propto -\frac{1}{HA\sigma\theta} \propto \frac{T}{D_b}\sigma^{-1} \tag{19}$$

$$\epsilon_T = \frac{\sigma}{H\theta^2} \propto \sigma \tag{20}$$

In the above equations, t_T is proportional to, and ϵ_T is inversely proportional to, applied stress. The above equations also predict that t_T decreases with increasing testing temperature T and the activation energy of t_T is for grain boundary diffusion, and that ϵ_T is independent of T. The results of Figs. 3 and 4 are consistent with the present model. The result in Fig. 5 is a little scattered, but the behaviour may agree with the present model.

The origin of transient and steady-state creep in metallic alloys has commonly been explained in terms of dislocation mechanisms [37, 38]. The dislocation creep may also occur in coarse-grained ceramics, e.g. in Al_2O_3 with a grain size of more than 10 μm [18, 39], and the formation of subgrain is observed in several ceramic materials (MgO, LiF, etc.) where the subgrain size is determined by imposed stress as well as metals [40, 41]. Primary creep in these ceramics may be explained in terms of dislocation activity and subgrain formation. However, no dislocation activity is observed in fine-grained Al_2O_3 at temperatures examined in this study in accordance with the previous reports [42, 43].

It is demonstrated that the transient region appears in diffusional creep and the transient strain is in the order of elastic strain [12, 44]. The elastic strain is estimated to be about 3×10^{-4} at 1150 °C and under applied stress of 100 MPa, which is much smaller than that observed in fine-grained Al_2O_3. The diffusional transient model proposed by Raj [10] also predicts that the time extent of transient stage is less than 1 ks for Al_2O_3 at 1150 °C, while the experimental t_T in the present Al_2O_3 is 45 ks at 1150 °C under the stress of 53 MPa. The difference is more than one order of magnitude.

Strain hardening during grain boundary sliding in fine-grained ceramics is sometimes explained in terms of grain growth [20, 45] or grain elongation [46]. However, there is no significant grain growth during creep testing in Al_2O_3 examined in this study as mentioned previously. Consequently, the grain growth is ruled out from a possible origin of primary creep in finer grained Al_2O_3.

Grain boundary sliding caused by dislocation glide in grain boundaries is another mechanism of high-temperature creep in metallic materials [47–49]. Ceramics without grain boundary glassy phase may also deform by the same mechanism. For example, Heuer *et al.* [43] observed extrinsic grain boundary dislocations in the crept Al_2O_3 with a grain size of 1.2 μm and the temperature of 1400 °C, which may be associated with grain boundary sliding. Extrinsic dislocations are also found in the grain boundaries of deformed single-phase Al_2O_3 [50, 51]. It may therefore be concluded that the transient creep in fine-grained Al_2O_3 is caused by grain boundary sliding which involves grain boundary dislocation glide and climb.

6. Conclusions

The transient creep behaviour of high-purity polycrystalline alumina has been examined at temperatures of 1150–1250 °C. The time extent of transient creep seems to be proportional to applied stress and to decrease with increasing temperature by an Arrhenius relation. The transient strain also seems to be proportional to applied stress.

A two-dimensional model of high-temperature creep caused by grain boundary sliding is proposed. The grain boundary sliding is assumed to occur by the glide of grain boundary dislocations accommodated by the climb of leading dislocation in pile-ups into the neighbouring grains. The model predicts a change in creep strain ϵ with time t as follows

$$\epsilon = a_1 t + a_2(1 - \exp(-a_3 t))$$

where the value of a_1 describes the steady-state strain rate $\dot{\epsilon}_s$, a_2 the total transient strain ϵ_T and a_3 the time extent of transient region. The time function has a similar form with that used for describing the experimental creep curves in metallic alloys. From the time function, the transient strain ϵ_T and the time extent of transient

region t_T are approximately given as a function of stress and temperature as follows

$$t_T \propto \frac{T}{D_b}\sigma^{-1}$$
$$\epsilon_T \propto \sigma$$

The stress dependence of t_T and ϵ_T estimated from the experimental creep curves in high-purity, fine-grained alumina is in accordance with that predicted from the model.

Acknowledgement

The authors wish to express their gratitude to the Ministry of Education, Science and Culture, Japan, for the financial support by a Grant-in-Aid for Developmental Scientific Research (2)–06555202 for Fundamental Scientific Research.

References

1. A. K. AMIN, A. K. MUKHERJEE and J. E. DORN, *J. Mech. Phys. Solids* **18** (1970) 413.
2. R. W. EVANS and B. WILSHIRE, "Creep of metals and alloys" (The Institute of Metals, London, 1985) p. 116.
3. H. E. EVANS and K. R. WILLIAMS, *Phil. Mag.* **25** (1972) 1399.
4. N. S. AKULAV, *Acta Metall.* **12** (1964) 1195.
5. J. C. M. LI, *ibid.* **11** (1963) 1269.
6. G. A. WEBSTER, *Phil. Mag.* **14** (1966) 775.
7. B. DERBY and M. F. ASHBY, *Acta Metall.* **35** (1987) 1349.
8. A. S. ARGON and A. K. BATTACHARYA, *ibid.* **35** (1987) 1499.
9. R. RAJ and M. F. ASHBY, *Metall. Trans.* **2** (1971) 1113.
10. R. RAJ, *ibid.* **A6** (1975) 1499.
11. H. J. FROST and M. F. ASHBY, "Deformation–mechanism maps" (Pergamon, Oxford, UK, 1982).
12. G. MALAKONDAIAH, N. PRASAD, G. SUNDARARAJAN and P. RAMA RAO, *Acta Metall.* **36** (1988) 2167.
13. G. L. REYNOLDS, W. B. BEERÉ and B. BURTON, *Metal Sci.* **11** (1977) 213.
14. P. GRUFFEL, P. CARRY and A. MOCELLIN, *Sci. Ceram.* **14** (1988) 587.
15. A. H. CHOKSHI and J. R. PORTER, *J. Mater. Sci.* **21** (1986) 705.
16. A. G. ROBERTSON, D. S. WILKINSON and C. H. CÁCERES, *J. Amer. Ceram. Soc.* **74** (1991) 915.
17. D. M. OWEN and A. H. CHOKSHI, *Scripta Metall. Mater.* **29** (1993) 869.
18. W. R. CANNON and O. D. SHERBY, *J. Amer. Ceram. Soc.* **60** (1977) 44.
19. A. H. CHOKSHI, *J. Mater. Sci.* **25** (1990) 3221.
20. Y. YOSHIZAWA and T. SAKUMA, *Acta Metall Mater.* **40** (1992) 2943.
21. Y. YOSHIZAWA, PhD Dissertation, University of Tokyo, Japan, 1993.
22. H. YOSHIDA, K. OKADA, Y. IKUHARA and T. SAKUMA, *Phil. Mag. Lett.* **76** (1997) 9.
23. Y. TAKIGAWA, Y. IKUHARA and T. SAKUMA, in "Materials science forum, superplasticity in advanced materials ICSAM-97," Vol. 243–245, Edited by A. H. Chokshi (Trans Tech Publications, Switzerland, 1997) p. 167.
24. P. G. MCVETTY, *Mech. Eng.* **56** (1934) 149.
25. F. GAROFALO, "Fundamentals of creep and creep-rupture in metals" (MacMillan, New York, 1970).
26. R. M. CANNON, W. H. RHODES and A. H. HEUER, *J. Amer. Ceram. Soc.* **63** (1980) 46.
27. M. L. GALL, B. LESAGE and J. BERNARDINI, *Phil. Mag. A* **70** (1994) 761.
28. D. PROT and C. MONTY, *ibid.* **73** (1996) 899.
29. B. BURTON, "Diffusional creep of polycrystalline materials" (Trans. Tech. Publ. Aedermannsdorf, Switzerland, (1977).
30. B. BURTON, *Mater. Sci. Eng.* **10** (1972) 9.
31. E. ARZT, M. F. ASHBY and R. A. VERRALL, *Acta Metall.* **31** (1983) 1977.
32. T. G. LANGDON, *Phil. Mag.* **22** (1970) 689.
33. R. C. GIFKINS, *Metall. Trans.* **A7** (1976) 1225.
34. A. ARIELI and A. K. MUKHERJEE, *Mater. Sci. Eng.* **45** (1980) 61.
35. J. P. HIRTH and J. LOTHE, "Theory of dislocations," (Wiley-Interscience Publication, New York 1982) p. 555, p. 774.
36. S. SAKAGUCHI, N. MURAYAMA, Y. KODAMA and F. WAKAI, *J. Mater. Sci.* **10** (1991) 282.
37. A. ORLOVÁ and J. CADEK, *Phil. Mag.* **28** (1973) 891.
38. H. HASEGAWA, R. HASEGAWA and S. KARASHIMA, *Trans. JIM* **11** (1970) 101.
39. A. CROSBY and P. E. EVANS, *J. Mater. Sci.* **8** (1973) 1573.
40. W. R. CANNON and T. G. LANGDON, *ibid.* **23** (1988) 1.
41. A. H. CHOKSHI and T. G. LANGDON, *Mater. Sci. Tech.* **7** (1991) 577.
42. J. D. FRENCH, J. ZHAO, M. P. HARMER, H. M. CHAN and G. A. MILLER, *J. Amer. Ceram. Soc.* **77** (1994) 2857.
43. A. H. HEUER, N. J. TIGHE and R. M. CANNON, *ibid.* **63** (1980) 53.
44. R. S. MISHRA, D. BANERJEE and A. K. MUKHERJEE, *Mater. Sci. Eng.* **A192/193** (1995) 756.
45. I-W. CHEN and L. A. XUE, *J. Amer. Ceram. Soc.* **73** (1990) 2585.
46. Z. C. WANG, N. RIDLEY and T. J. DAVIES, *J. Mater. Sci. Lett.* **14** (1995) 355.
47. O. A. KAIBYSHEV, R. Z. VALIEV and A. K. EMALETDINOV, *Phys. Status Solidi* **A90** (1985) 197.
48. R. Z. VALIEV, V. YU. GERTSMAN and O. A. KAIBYSHEV, *ibid.* **A97** (1986) 11.
49. R. I. TODD, in "Superplasticity: 60 years after Person," edited by N. Ridley (Institute of Materials, London, 1995) p. 33.
50. L. PRIESTER and S. LARTIGUE, *J. Eur. Ceram. Soc.* **8** (1991) 47.
51. S. LARTIGUE and L. PRIESTER, *J. Amer. Ceram. Soc.* **71** (1988) 430.

Received 19 June
and accepted 21 July 1998